ORIGINAL ARTICLE

A C G publications

Rec. Nat. Prod. 17:3 (2023) 522-528

records of natural products

A Previously Undescribed Cleistanthane-Type Diterpenoid from *Peniophora incarnate*

Mei-Mei Li [#1], Wen-Xiu Guo [#1], Yu Jiang [#2], Cong-Cong Li [1], Xue-Yan Huo [1], Yun-Jie Hu [1], Da-Le Guo [1], Li-Jun Huang [*1,3] and Yun Deng [*1]

[1] *State Key Laboratory of Southwestern Chinese Medicine Resources, Chengdu University of Traditional Chinese Medicine, Chengdu 611137, People's Republic of China*
[2.] *Department of Nursing, Sichuan Nursing Vocational College，Chengdu 611137, China*
[3] *School of Basic Medical Sciences, Chengdu University of Traditional Chinese Medicine, Chengdu 611137, People's Republic of China*

(Received October 31, 2022; Revised December 01, 2022; Accepted December 08, 2022)

Abstract: A newly discovered cleistanthane-type diterpenoid named incarnatin A (**1**) was isolated from *Peniophora incarnate*, an endophytic fungus obtained from the roots of *Ligusticum chuanxiong*. Its absolute configuration was unambiguously elucidated by spectroscopic means including HRMS and NMR combined with ECD calculations. Transcriptome sequencing indicated that **1** could inhibit angiogenesis.

Keywords: Cleistanthane; incarnatin A; structure elucidation; transcriptome sequencing; angiogenesis.

1. Introduction

The genus *Peniophora* is a rich resource of auspicious natural products. Phytochemical investigation of several *Peniophora* species led to the isolation of chlamydocin [1], benzaldehyde derivatives [2], xanthone [3-4] as well as sesquiterpenes [5]. As a part of our search for secondary metabolites with structural novelty or bioactivity from endophytes of Chinese medicines in the southwest of China [6-10], *Peniophora incarnate* was obtained as an endophytic fungus from the roots of *Ligusticum chuanxiong*. Subsequent chemical investigation resulted in the isolation of incarnatin A (**1**), a previously undescribed cleistanthane-type diterpenoid whose structure was elucidated by comprehensive analyses of spectroscopic evidence from HRMS, NMR, as well as ECD calculations. Transcriptome sequencing (*RNA-Seq*) was subsequently applied to analyze the potential function of **1**. Herein, the details of isolation, structural elucidation, and *RNA-Seq* results of **1** are reported.

[*] Corresponding author: E-mail: huanglj27@cdutcm.edu.cn (Li-Jun Huang); E-mail: dengyun@cdutcm.edu.cn (Yun Deng).

[#] Mei-Mei Li and Wen-Xiu Guo contributed equally to this work.

The article was published by ACG Publications
http://www.acgpubs.org/journal/records-of-natural-products May-June 2023 EISSN:1307-6167
DOI: http://doi.org/10.25135/rnp.374.2210.2619
Available online :January 19, 2023

2. Materials and Methods

2.1. Instruments and Materials

Optical rotation was measured with a Perkin Elmer Model 241 polarimeter (Perkin Elmer, Inc., MA, USA). Ultraviolet spectrum was obtained on a Perkin Elmer Lambda 35 UV-VIS spectrometer (Perkin Elmer, Inc., MA, USA). Infrared spectrum was collected on a PerkinElmer one FT–IR spectrometer (Perkin Elmer, Inc., MA, USA) with KBr disks. The circular dichroism spectrum was collected on a Chirascan CD spectrometer (Applied Photophysics Lid., Leatherhead, UK). The 1D and 2D NMR data were recorded on a Bruker Ascend 700-MHz spectrometer (Bruker, MA, USA), and HRESIMS was collected on a Q Exactive UHMR Hybrid Quadrupole-Orbitrap mass spectrometer (Thermo Fisher Scientific, MA, USA). Column chromatography was performed using macro-porous resin D101 (Yunkai Sci. & Tech., Tianjin, China) as well as RP-18 silica gel (300-400 mesh, Welch, Shanghai, China). The semi-preparative HPLC was conducted on an NP7000 series instrument (Hanbang Sci. & Tech., China) using an Ultimate PFP-C_{18} column (4.6×250 mm, 5 μm) (Welch Technology, China).

2.2. Fermentation and Extraction

Peniophora incarnate was isolated from the root of *Ligusticum chuanxiong*, which was collected from the suburbs of Pengzhou City, Sichuan Province, P. R. China. It was identified by morphological observation combined with a sequence analysis of the ITS region of the rDNA. The strain (GenBank accession number DQ513513) was firstly incubated in a M1 liquid medium at 30 °C and 120 r/min for 7 days, then cultivated on a 5 kg scale brown rice medium using one hundred 330 mL tissue culture flasks containing 2 g of peptone, 40 g of brown rice, 25 mL of water and 10 mL of seed culture for 30 days at room temperature.

The fermentation broth was extracted three times with 10 L of methanol using ultrasonic extraction. Then the extract was concentrated under reduced pressure to yield a semi-fluid, which was dispersed in 55 °C water and extracted with the same volume of ethyl acetate. The extract was concentrated again to obtain a 32.4 g sample for subsequent separation and purification.

2.3. Separation and Purification

The foresaid sample was separated into four fractions using a macro-porous resin, D101 (80 mm × 1500 cm, d × L, eluting stepwise with a MeOH-H_2O of 0:100, 30:70, 60:40, and 95:5). The fraction 60: 40 was further separated using RP-18 silica gel (300-400 mesh, 49 mm × 300mm , d × L), eluting stepwise with MeOH-H_2O from 50:50 to 100:0 to yield sixteen sub-fractions. Sub-fraction three was further fractionated by preparative HPLC using a reverse-phase column to afford incarnatin A (MeOH-H_2O, 70:30; 3 mL/min; t_R: 18.35 min; 5.72 mg).

Incarnatin A ***(1)***: White powder; $[\alpha]_D^{25}$ = −4.839 (*c* = 0.062, MeOH); UV (MeOH): λ_{max} = 196 (1.58); IR (KBr) ν_{max}: 3429, 2927, 2854, 1740, 1716, 1593, 1381, 1241, 1041 cm^{-1}; HRESIMS *m/z* 413.1934 $[M+Na]^+$ (calcd. 413.1935); ^1H NMR and ^{13}C NMR data see Table 1.

2.4. ECD Calculations

The theoretical calculation of **1** was performed using Gaussian 16 (Gaussian Inc., Wallingford, CT). Conformational analysis was first conducted using Conflex 8 to generate conformations (search limit: 5 Kcal/mol) [7]. Possible conformers were optimized using TDDFT at the B3LYP/6-31G (d, p) level in gas, then at ωB97XD/DGDZVP in methanol [8]. The ECD spectra were derived by weighing the Boltzmann distribution rate of each geometric conformer. SpecDis 1.71 was used to sum the single CD spectra after Boltzmann statistical weighting to generate the Gauss curve (0.3 eV) and comparison with experimental data [9-11].

2.5 Transcriptome Sequencing (RNA-Seq)

RAW 264.7 macrophages were seeded into 6-well plates. When cells achieved a density of 60-70%, they were pre-treated with 1 at a concentration of 60 μM or without **1** and divided into two groups (the CK group and the incarnatin A group). Cells were collected and lysed with RNA Isolator Total RNA Extraction Reagent (Invitrogen, USA). Total RNA samples were purified, concentrated, and evaluated for integrity to establish a cDNA library. An Illumina HiSeq X Ten sequencer was used to conduct *RNA-seq*. Quality control of raw data was conducted using the FastQC tool. The clean reads were separately compared with the reference genome using HISAT2 software. Differential expression of genes (DEGs) was assessed using the DESeq2 R package. DEGs with absolute fold change ≥2 and p adjusted value <0.05 were considered as significantly differentially expressed genes. GO enrichment analysis and KEGG pathway enrichment analysis were performed using the clusterProfiler R package. The gene sets used for GSEA analysis were obtained from the GSEA website (http://www.gsea-msigdb) and the data visualization was performed using Hiplot software.

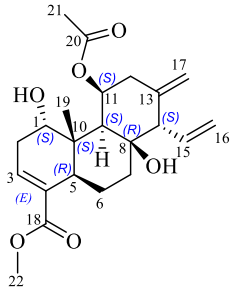

Figure 1. Chemical structure of incarnatin A (**1**)

3. Results and Discussion

3.1. Structure Elucidation

Incarnatin A (**1**) was isolated as a white powder. Its molecular formula was assigned as $C_{22}H_{30}O_6$ by a pseudo-molecular ion peak in HRESIMS. Its ^{1}H NMR, and HMQC spectra indicated the presence of olefinic protons at δ 6.40 (H-3), 5.98 (H-15), 5.11(H-16a), 5.08 (H-16b), 4.88 (H-17a), 4.79 (H-17b); oxygenated methines at δ 5.44 (H-11), 4.92(H-1); oxygenated methyl at δ 3.61 (H-22); methylenes at δ 2.49 (H-12α), 2.37 (H-2β), 2.22 (H-12β), 2.05 (H-2α), 1.92 (H-6α), 1.60 (H-7α), 1.48 (H-6β), and 1.38 (H-7β); and methines at δ 2.72 (H-14), 2.25 (H-5), 2.02 (H-9). The ^{13}C NMR spectrum of **1** displayed 22 carbons including ester carbons at δ 169.4 (C-20) and 167.8 (C-18); olefinic carbons at δ 143.3 (C-13), 137.3 (C-15), 134.3 (C-3), 132.7 (C-4), 117.2 (C-16), 113.7 (C-17); oxygenated methines at δ 69.7(C-1), 69.5 (C-11); oxygenated methyl at δ 51.2 (C-22); methylenes at δ37.0 (C-7), 36.5 (C-12), 31.3 (C-2), 18.4 (C-6); and methines at δ 63.4(C-14), 41.8(C-9), 39.5(C-5).

The ^{1}H-^{1}H COSY correlations of H-1/H-2/H3, of H-5/H-6/H-7, of H-9/H-11/H-12, H-14/H-15/H-16 as well as HMBC correlations of H-19/C-1, C-9, C-10, C-5, of H-5/C3, of H-6/C-4, of H-7/C-8, C-9, of H-17/C-13, C-12, C-14 and of H-14/C-8, C-9 establishes a typical cleistanthane diterpenoid moiety (Figure 2A). The planar structure of compound **1** was confirmed by the HMBC correlations of H-22/C-4, H-21/C-11. The relative configuration of compound **1** was deduced to be 1*S**, 5*R**, 8*R**, 9*S**, 10*S**, 11*S**, 14*S** by the NOESY correlations of H-1/H-19, H-19/H-2β, H-19/8-OH, H-11/H-1, H-14/H-7β (Figure 2B). Since the calculated ECD curve of 1*S*,5*R*,8*R*,9*S*,10*S*,11*S*,14*S*-**1** matches the experimental spectrum exactly. As shown in Figure 1, compound 1 has finally been confirmed in its absolute configuration.

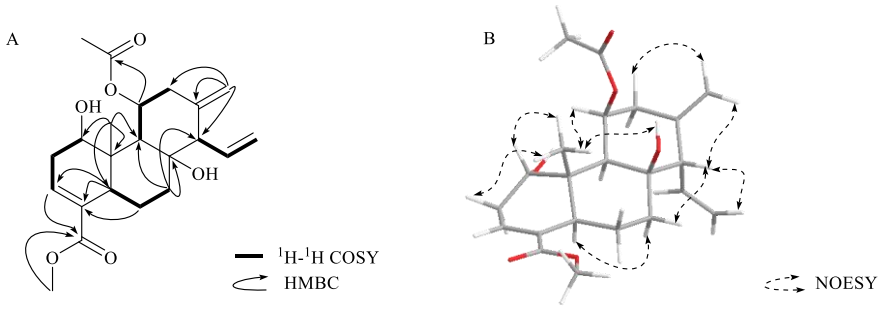

Figure 2. A. Key HMBC (arrows) and ^{1}H-^{1}H COSY (bold) correlations of compound **1**; B. Key NOESY correlations (double arrows) of compound **1**

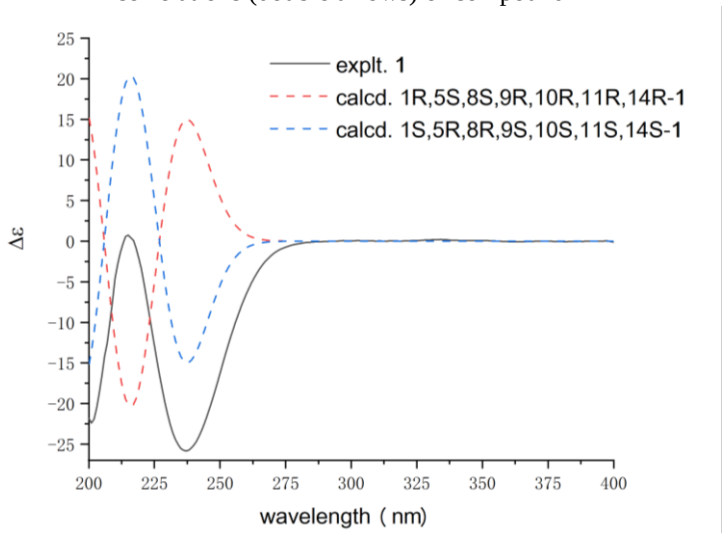

Figure 3. Calculated ECD spectra and experimental ECD curve of compound **1**

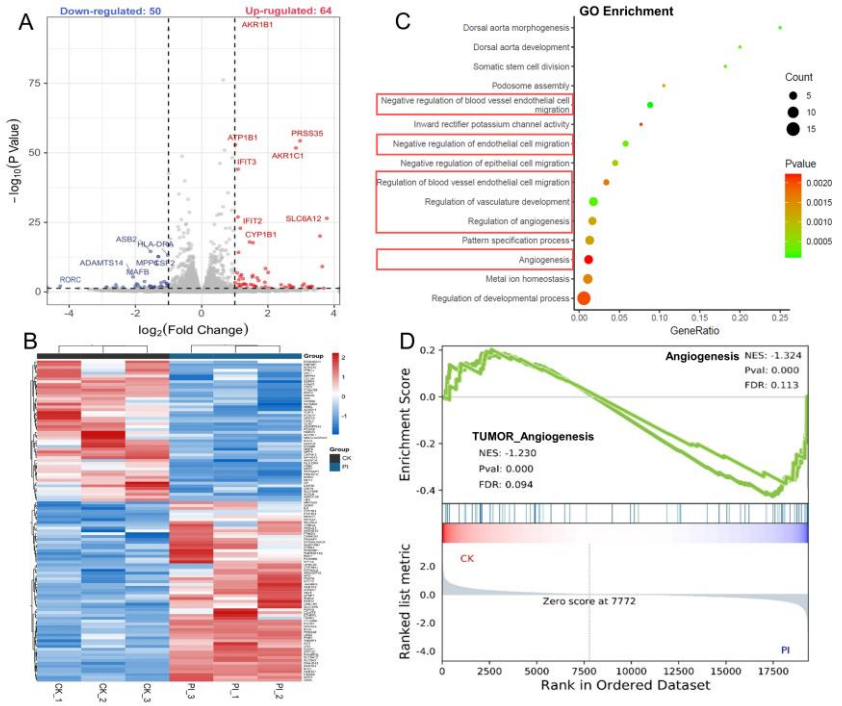

Figure 4. The result of RNA sequencing. (A) The volcano plot of DEGs between pre-treated with or without **1**; The red and blue dots represent significantly up-regulated and down-regulated genes, respectively. Grey dots indicate genes with no significant variation. (B) Heatmap of 114 common DEGs in DMSO and **1** pre-treated RAW264.7 macrophages. (C) GO enrichment results for DEGs. (D) GSEA analysis. The DEGs were defined by |foldchange| ≥2 and p adjusted value <0.05.

Table 1. The NMR spectroscopic data of compound **1** (700MHz, DMSO-d_6)

No.	δ_H	δ_C	^1H-^1H COSY	HMBC
1	3.59 (1H, s)	69.7	2	3, 5, 9
2	2.37 (1H, m), 2.05 (1H, m)	31.3	3	1, 3, 4, 10
3	6.40 (1H, m)	134.3	2	1, 2, 5, 18
4		132.7		
5	2.25 (1H, m)	39.5	6	3, 4, 19
6	1.92 (1H, d, 11.1) 1.48 (1H, dd, 12.7, 3.1)	18.4	7	4, 7, 8
7	1.60 (1H, m) 1.38 (1H, dt, 13.4, 3.0)	37.0	6	5, 6, 8, 9
8		75.2		
9	2.02 (1H, d, 2.1)	41.8	11	8, 10, 11, 19
10		40.4		
11	5.44 (1H, m)	69.5	9, 12	8, 9, 12, 13, 20
12	2.49 (1H, m), 2.22 (1H, m)	36.5	11, 17	9, 11, 13, 14, 17
13		143.3		
14	2.72 (1H, d, 9.3)	63.4	15	8, 9, 12, 13, 15
15	5.98 (1H, dt, 16.8, 9.9)	137.3	14, 16	8, 13, 14
16	5.11 (1H, dd, 16.8, 1.5) 5.08 (1H, dd, 10.2, 2.1)	117.2	15	13, 14, 15
17	4.88 (1H, s); 4.79 (1H, s)	113.7	12	12, 13, 14
18		167.8		
19	0.93 (3H, s)	15.0		1, 5, 9, 10
20		169.4		
21	2.00 (3H, s)	21.4		20, 11
22	3.62 (3H, s)	51.2		18, 4
1-OH	4.92(1H, s)			
8-OH	3.17(1H, s)			7, 8, 9

3.2. RNA-Seq Analysis

RAW264.7 macrophages were pre-treated with DMSO and small molecule **1** for 24 h and the cells were collected for transcriptome analysis to reveal the biological activity of **1**. Genome-wide profiles of differentially expressed genes (DEGs) were obtained by RNA sequencing, and the results are shown in Figure 4. A total of 114 DEGs were observed in the volcano plot of RNA sequencing (Figure 4A). Many of the downregulated DEGs were the ones that particularly interested us. For example, the down-regulated RORC gene as an orphan nuclear receptor gene interferes with angiogenesis through the regulation of vascular endothelial cells [12]. And the ADAMTS14 gene can activate vascular endothelial growth factor [13,14]. Excitingly, heat map of 114 DEGs pre-treated with DMSO and **1**, which exhibited different gene signatures in the CK and **1** group (Figure 4B). This was a further suggestion that **1** may possess some significant biological activity. Furthermore, gene ontology (GO) enrichment analysis was performed on 50 down-regulated DEGs that regulated several biological processes associated with vascular endothelial migration and angiogenesis (Figure 4C). Further gene set enrichment analysis (GSEA) showed that the normalized enrichment score (NES) of angiogenesis and tumor angiogenesis is less than -1, q value less than 0.001, and FDR less than 0.25 (Figure 4D). There was a significant reduction in angiogenesis and tumor angiogenesis-related biological processes in the 1 treatment group in comparison with the control group. These also suggest that **1** has a potential negative regulatory effect on angiogenesis and tumor angiogenesis.

Acknowledgments

This work was supported by the Department of Science and Technology of Sichuan Province (2021YFN0134), Chengdu University of Traditional Chinese Medicine (CZYJC1905) and the National Interdisciplinary Innovation Team of Traditional Chinese Medicine (ZYYCXTD-D-202209).

Supporting Information

Supporting Information accompanies this paper on http://www.acgpubs.org/journal/records-of-natural-products

ORCID
Mei-Mei Li: 0000-0001-5492-3263
Wen-Xiu Guo: 0000-0001-6511-4656
Yu Jiang: 0000-0002-6645-3315
Cong-Cong Li: 0000-0001-9713-0271
Xue-Yan Huo: 0000-0003-0217-4090
Yun-Jie Hu: 0000-0001-7282-6993
Da-Le Guo: 0000-0003-3219-7066
Li-Jun Huang: 0000-0003-0563-6684
Yun Deng: 0000-0002-3428-8992

References

[1] H. Tani, Y. Fujii, and H. Nakajima (2001). Chlamydocin analogues from the soil fungus *Peniophora* sp: structures and plant growth-retardant activity, *Phytochemistry* **58**, 305–310.

[2] W. A. Ayer, and L. S. Trifonov (1993). Metabolites of *Peniophora polygonia*, part 2. Some aromatic compounds, *J. Nat. Prod.* **56**, 85–89.

[3] A. Hartl, A. Stelzner, M. Ritzau, S. Heinze, and U. Grafe (1998). 5-hydroxy-3,4,7-triphenyl-2,6-benzofurandione, a new xanthine oxidase inhibitor from *Peniophora sanguinea*, *J. Antibiot.* **51**, 528–530.

[4] S. J. Li, F. W. Jiao, W. Li, X. Zhang, W. Yan, and R. H. Jiao (2020). Cytotoxic xanthone derivatives from the mangrove-derived endophytic fungus *Peniophora incarnate* Z4, *J. Nat. Prod.* **83**, 2976–2982.

[5] W. A. Ayer, and L. S. Trifonov (1992). Drimane sesquiterpene lactones from *Peniophora polygonia*, *J. Nat. Prod*. **55**, 1454–1461.

[6] Q. X. Kuang, L. R. Lei, Q. Z. Li, W. Peng, Y. M. Wang, Y. F. Dai, D. Wang, Y. Deng, and D. L. Guo (2022). Investigation of the anti-inflammatory activity of fusaproliferin analogues guided by transcriptome analysis, *Front. Pharmacol*. **13**, 881182.

[7] Y. M. Cao, D. L. Guo, M. Y. Jin, L. Tan, T. L. Yang, F. Deng, Y. C. Gu, X. H. Li, Z. X. Cao, and Y. Deng (2021). Two new nor-sesquiterpenoids from *Fusarium tricinctum*, an endophytic fungus isolated from *Ligusticum chuanxiong*, *Nat. Prod. Res.* **35**, 3535–3539.

[8] D. L. Guo, L. Qiu, D. Feng, X. He, X. H. Li, Z. X. Cao, Y. C. Gu, L. Mei, F. Deng, and Y. Deng (2020). Three new α-pyrone derivatives induced by chemical e1genetic manipulation of *Penicillium herquei*, an endophytic fungus isolated from *Cordyceps sinensis*, *Nat. Prod. Res.* **34**, 958–964.

[9] F. Ju, Q. X. Kuang, Q. Z. Li, L. J. Huang, W. X. Guo, L. Q. Gong, Y. F. Dai, L. Wang, Y. C. Gu, D. Wang, Y. Deng, and D. L. Guo (2021). Aureonitol analogues and orsellinic acid esters isolated from *Chaetomium elatum* and their antineuroinflammatory activity, *J. Nat. Prod.* **84**, 3044–3054.

[10] J. Yan, W. X. Guo, L. Y. Zhou, Z. X. Cao, J. Pei, Y. Deng, B. Li, D. Liu, D. L. Guo, and C. Peng (2022). A neoprzewaquinone analogue from *Salvia miltiorrhiza* Bunge, *Rec. Nat. Prod.* **16**, 572–578.

[11] M.Zhao, G. Chen, G. Chen, T.T. Lin and Y.Lu (2020). A new labdane diterpene from the aerial parts of *Chloranthus serratus*, *Rec. Nat. Prod*. **14**, 378–382.

[12] Q. X. Kuang, Y. Luo, L. R. Lei, W. X. Guo, X. A. Li, Y. M. Wang, X. Y. Huo, M. D. Liu, Q. Zhang, D. Feng, L. J. Huang, D. Wang, Y. C. Gu, Y. Deng, and D. L. Guo (2022). Hydroanthraquinones from *Nigrospora sphaerica* and their anti-inflammatory activity uncovered by transcriptome analysis, *J. Nat. Prod*. **85**, 1474–1485.

[13] M. Turkoglu, S. Kilic, E. Pekmezci and M. Kartal (2018). Evaluating Antiinflammatory and Antiandrogenic Effects of Garden Cress (Lepidium sativum L.) in HaCaT cells, *Rec. Nat. Prod.* **12**, 595-601.

[14] L. J. Huang, Y. M. Wang, L. Q. Gong, C. Hu, Y. Gui, C. Zhang, X. Tan, X. K. Yu, Y. L. Liao, Y. Luo, Y. Q. Tang, Y. F. Dai, Y. Deng, D. Wang, and D. L. Guo (2022). N-acetyldopamine dimer attenuates DSS-induced ulcerative colitis by suppressing NF-κB and MAPK pathways, *Front. Pharmacol*. **13**, 842730.